CRC Report No. A-128

Quantifying the effects of VOC/ NOx chemistry on tropospheric ozone production: Yields of organic nitrates from reaction of substituted organic peroxy radicals with NO.

Draft Final Report

April 2025

COORDINATING RESEARCH COUNCIL, INC.
1 CONCOURSE PARKWAY• SUITE 800 • ATLANTA, GA 30328

The Coordinating Research Council, Inc. (CRC) is a non-profit corporation supported by the petroleum and automotive equipment industries with participation from other industries, companies, and governmental bodies on research programs of mutual interest. CRC operates through the committees made up of technical experts from industry and government who voluntarily participate. The five main areas of research within CRC are: air pollution (atmospheric and engineering studies); aviation fuels, lubricants, and equipment performance; heavy-duty vehicle fuels, lubricants, and equipment performance (e.g., diesel trucks); light-duty vehicle fuels, lubricants, and equipment performance (e.g., passenger cars); and sustainable mobility (e.g., decarbonization). CRC's function is to provide the mechanism for joint research conducted by industries that will help in determining the optimum combination of products. CRC's work is limited to research that is mutually beneficial to the industries involved. The final results of the research conducted by, or under the auspices of, CRC are available to the public.

LEGAL NOTICE

This report was prepared by the University Corporation for Atmospheric Research (UCAR) as an account of work sponsored by the Coordinating Research Council (CRC). Neither the CRC, members of the CRC, UCAR, nor any person acting on their behalf: (1) makes any warranty, express or implied, with respect to the use of any information, apparatus, method, or process disclosed in this report, or (2) assumes any liabilities with respect to use of, inability to use, or damages resulting from the use or inability to use, any information, apparatus, method, or process disclosed in this report. In formulating and approving reports, the appropriate committee of the Coordinating Research Council, Inc. has not investigated or considered patents which may apply to the subject matter. Prospective users of the report are responsible for protecting themselves against liability for infringement of patents.

Quantifying the effects of VOC/NOx chemistry on tropospheric ozone production: Yields of organic nitrates from reaction of substituted organic peroxy radicals with NO.

John J. Orlando, Geoffrey S. Tyndall, Qing Ye, Frank Flocke, Paul J. Ziemann, Emmy Longnecker and Anna Ziola
Atmospheric Chemistry Observations and Modeling Laboratory
National Center for Atmospheric Research (NCAR), Boulder CO USA.
University of Colorado (CU), Boulder CO USA.

EXECUTIVE SUMMARY

The objective of this project has been to improve the state of knowledge regarding the yields of organic nitrates in volatile organic compound (VOC) oxidation, and thus to further constrain model representation of the effects of VOC/NOx chemistry on ozone and secondary organic aerosol (SOA) production. Nitrate production occurs from the reaction of organic peroxy radicals (abbreviated as RO_2, where R is an organic fragment) with NO, in parallel with chemistry that generates NO_2 and hence ozone; thus, yields of the nitrates are anti-correlated with local ozone production.

$RO_2 + NO \rightarrow RO + NO_2$ Branching ratio $(1-\alpha)$
$RO_2 + NO \rightarrow RONO_2$ Branching ratio (α)
$NO_2 + hn\ (+ O_2) \rightarrow NO + O_3$

The focus of a previous CRC-funded project carried out by our group at NCAR was to determine nitrate yields (α in the equations above) and hence ozone and SOA production in the chemistry of 'simple' alkanes, species containing only C- and H-atoms. In this study, the focus has been on the determination of nitrate yields in the atmospheric chemistry of oxygenated VOCs (OVOCs) such as ethers, esters, carbonyls, and a di-ether, compounds that (unlike the alkanes) have oxygen-containing functional groups. These types of compounds are typically present in the atmosphere as a result of human activity, either as direct emissions or as a result of conversion of these emissions to more oxidized species.

Laboratory determinations of nitrate production yields in the oxidation of these classes of OVOC species have to date only been sporadic. This dearth of nitrate yield data leaves gaps and uncertainties in atmospheric chemistry models and mechanisms used in the study of urban air quality; depending on the model/mechanism, these processes are often not represented at all, are implemented as for the alkanes, or are implemented to the extent possible based on the limited information currently available. Resultant potential systematic biases in NOx lifetime and atmospheric oxidative capacity in the models can then lead to concomitant uncertainty in the production of secondary pollutants such as ozone and SOA, and potential errors in mitigation strategies developed to reduce pollutant formation.

The work conducted herein can be divided into two major sections – the first a detailed study of di-octyl ether (DOE), C_8H_{17}-O-C_8H_{17}, conducted at University of Colorado -Boulder (CU), the second a set of less detailed studies of an array of smaller oxygenated VOC species (including ethers, esters and carbonyls), focusing on nitrate production yield determinations, carried out at NCAR. The studies were conducted in environmental chambers at each location, each equipped with appropriate (but different) analytical capabilities. *The overarching finding of the study is that, in all cases studied, the yield of organic nitrate from the oxidized species is lower than has been found to be the case for an alkane of similar size. As nitrate production is anti-correlated with ozone production, these reduced nitrate yields imply higher local production of ozone from the oxygenated VOC species than for a corresponding alkane**.*** More details associated with each of these two studies are given below.

1) Study of DOE Oxidation (CU)

The DOE oxidation study was carried out in the Ziemann group atmospheric chamber located at CU, using OH radicals to initiate the oxidation process. It is found, rather remarkably, that the presence of the single O-atom in DOE has a profound impact on the outcome of the chemistry, with 78% of the chemistry modified compared to that occurring in a similar-sized alkane (e.g., hexadecane $C_{16}H_{34}$). One major impact of the presence of the ether group is that the oxidation leads to the occurrence of more fragmentation during the oxidation process. More specifically, the major product of the oxidation is octyl formate, C_8H_{17}-O-CH=O, (yield $\approx$ 55%) which is formed by essentially splitting the parent DOE into two similarly sized fragments. This increased fragmentation results in *an overall decrease in the SOA production relative to an alkane of similar size.*

In addition, the overall nitrate production yield in the oxidation of DOE is found to be 15%, about half the amount formed in the oxidation of a similar sized alkane. This factor of two decrease is traced directly to the presence of the ether linkage in the molecule. More than half of the OH reaction with DOE occurs on the two carbon atoms adjacent to the O-atom, and it is found that very little nitrate results from the specific organic peroxy radical formed via this pathway. As stated above, this reduced nitrate yield implies larger local ozone production from the large ether than from an alkane species like hexadecane.

2) Studies of Smaller Oxygenated VOCs (NCAR)

Numerous smaller organics were studied (albeit in less detail) at NCAR, including two ethers, a di-ether, two ketones and an ester, each containing 3-6 carbon atoms and 5-7 heavy (C and O) atoms. Oxidation of each species was initiated in the NCAR chamber via its reaction with Cl-atoms, which serves as an OH surrogate. Analytical tools used to quantify products included in situ FTIR spectroscopy and GC-FID. A summary of key findings:

a) Nitrate yields are found for all molecules studied to be considerably less, by at least a factor of two and up to about an order of magnitude, than from alkanes containing a similar number of heavy atoms. Thus, as presented above, local ozone production from oxidation of these types of OVOCs will be larger than is the case for a similarly sized alkane. The work, which directly focused on nitrate yields from these OVOCs, extends and supports a limited number of previous reports in the literature.

b) For diethyl ether, as was the case with DOE discussed above, the major reduction in nitrate formation is occurring due to chemistry occurring adjacent to the oxygenated functional group.

c) One can see a trend in nitrate formation yields for ethers that extends from about 1% in diethyl ether to 15% in DOE (versus 8% to 30% for similarly sized alkanes). The higher overall yield from DOE is due to the presence in this molecule of CH_2 groups located at a distance from the ether linkage.

d) In addition to the nitrate yield data, a few observations were made that point to inconsistencies in some reaction pathways in detailed atmospheric chemistry mechanisms and mechanism-generating systems. For example, the observation of acetic anhydride from oxidation of ethyl acetate (consistent with previous studies in our laboratory) is not captured in any model that we are aware of. Collectively, the data set obtained here should be useful in refining detailed models of atmospheric chemistry (e.g., the Leeds/York MCM, GECKO-A, and SAPRC Mech-Gen).

e) In an overall sense, extension of and decreased uncertainty associated with the data reported here could be obtained via: a) synthesis of as many multifunctional nitrates as possible, to obtain more accurate calibration of their yields and more precise measurements of wall losses, and b) extension of these studies to 'mid-size' compounds (e.g., molecules intermediate in size to dipropyl and dioctyl ether) to better establish trends.

BACKGROUND AND OBJECTIVE

The formation of atmospheric secondary pollutants, including ozone and secondary organic aerosol (SOA), is driven by non-linear chemistry involving volatile organic compounds (VOCs) and oxides of nitrogen (NOx). Direct control on ozone formation occurs via the reaction of organic peroxy radicals with NO. The peroxy radicals (RO_2), generated following reaction of OH with a VOC compound (RH), react with NO via two pathways, the first major channel generating ozone (via NO_2 photolysis) and the second limiting ozone formation via organic nitrate ($RONO_2$) production.

$$OH + RH\ (+ O_2) \rightarrow RO_2 + H_2O$$

$$RO_2 + NO \rightarrow RO + NO_2 \text{ (major channel, branching ratio } 1-\alpha)$$

$$RO_2 + NO + M \rightarrow RONO_2 + M \text{ (minor channel, branching ratio } \alpha)$$

$$NO_2 + h\nu\ (+ O_2) \rightarrow NO + O_3$$

Thus, quantification of the organic nitrate formation yields for the full range of VOCs, temperature and pressure conditions encountered in the troposphere is of critical importance in constraining model uncertainty regarding tropospheric ozone production and determining the efficacy of NOx vs VOC controls on ozone production.

Organic nitrate yields from the oxidation of alkanes have been reasonably well studied and demonstrate the inherent complexity – nitrate yields depend on the size of the peroxy radical, as well as on temperature and total pressure [*Orlando and Tyndall, 2012*; *Jenkin et al., 2019*]. In general, the organic nitrate production yield [α in the equations above] increases with the size of the peroxy radical under consideration, from a yield of less than 1% for CH_3O_2, to about 30% for peroxy radicals derived from dodecane (i.e., $C_{12}H_{25}O_2$) and larger alkanes, for example [*Arey et al., 2001; Yeh and Ziemann, 2014*]. Branching ratios to nitrate production are also believed to increase with decreasing temperature, although our recent CRC-funded work on alkane oxidation (as well as previous studies of cyclohexane in our laboratory [Orlando et al., 2000]) point to a weaker dependence on temperature than previously believed *[Tyndall et al., 2025, in preparation]*. The degree of branching at the site of the peroxy radical carbon has also been thought to influence the nitrate yield, with yields from secondary radicals [e.g., $CH_3\text{-}CH(OO\bullet)CH(CH_3)_2$] thought to exceed those from primary [e.g., $CH_2(OO\bullet)\text{-}CH_2CH(CH_3)_2$] or tertiary [e.g., $CH_3\text{-}CH_2C(OO\bullet)(CH_3)_2$] radicals of the same size by factors of two to three. However, our recent work points to these previous conclusions being incorrect; we have found nitrate yields that are indistinguishable for peroxy radicals of the same size, regardless of their structure – e.g., nitrate yields from each of the primary, secondary and tertiary radicals generated following OH oxidation of 2-methyl butane were shown to be essentially identical *[Tyndall et al., 2025]*.

Organic nitrate production in the OH-initiated oxidation of alkenes has also been the subject of a number of laboratory studies *[e.g., Matsunaga and Ziemann, 2009, 2010a; Teng et al., 2015; Bakker-Arkema and Ziemann, 2021a,b]*. The OH reaction with alkenes occurs via addition, thus the peroxy radicals of interest are hydroxy-substituted peroxy radicals, e.g., for 1-butene:

$$OH + CH_2{=}CHCH_2CH_3 \rightarrow HOCH_2\text{-}CH\bullet\text{-}CH_2CH_3$$

$$HOCH_2\text{-}CH\bullet\text{-}CH_2CH_3 + O_2 \rightarrow HOCH_2\text{-}CH(OO\bullet)\text{-}CH_2CH_3$$

$$HOCH_2\text{-}CH(OO\bullet)\text{-}CH_2CH_3 + NO \rightarrow HOCH_2\text{-}CH(O\bullet)\text{-}CH_2CH_3 + NO_2$$

$$HOCH_2\text{-}CH(OO\bullet)\text{-}CH_2CH_3 + NO \rightarrow HOCH_2\text{-}CH(ONO_2)\text{-}CH_2CH_3$$

Literature values for the nitrate yields reported for these systems are variable, but appear on average to be reduced somewhat from those found for the alkanes of similar size.

The chemical nature of VOCs emitted to the atmosphere extends well beyond just the alkanes and alkenes, however, and includes partially oxidized species (here designated as oxygenated VOCs, or OVOCs) such as alcohols, ethers, aldehydes, ketones, esters and organic acids. A subset of these species (including multi-functional species) are also formed *in situ* in the oxidation of the alkanes and alkenes *[e.g., Calvert et al., 2015]*. To date, however, only limited information is available regarding nitrate yields from the chemistry of these OVOCs. In the most direct study, *Espada and Shepson [2005]* found that nitrate yields for a variety of ethers and glycol ethers were reduced by approximately a factor of 2-4 from those obtained from alkanes of comparable size and structure. Studies of nitrate production from other OVOCs (esters, carbonyls), as summarized in *Jenkin et al.* [*2019*], are very limited and not conducted in a systematic fashion or with a direct focus on quantifying nitrate production, but generally show reduced nitrate yields relative to those expected from comparably sized alkanes.

This dearth of data on organic nitrate yields from oxidation of OVOCs leads to potential systematic uncertainties in atmospheric models used in the study of air quality; depending on the model/ mechanism, these processes are often not represented at all, are implemented as for the alkanes, or are implemented to the extent possible based on the limited information summarized above. Resultant potential systematic biases in NOx lifetime and atmospheric oxidative capacity in the models can then lead to concomitant uncertainty in the production of secondary pollutants such as ozone and SOA, and potential errors in mitigation strategies developed to reduce pollutant formation.

Thus, in this work, we have conducted determinations of nitrate production from the oxidation of various OVOC (i.e., from the reaction of substituted RO_2 with NO). Types of molecules studied include ethers, esters, ketones, and a multi-functional ether. The studies were conducted in environmental chambers at NCAR and CU-Boulder, with appropriate (but different) analytical capabilities associated with each chamber.

LABORATORY METHODS

In general, our experiments are conducted by photolyzing mixtures of gases comprised of the following: an organic nitrite (used as a source of OH) or Cl_2 (a source of Cl-atoms, which act as OH surrogates); the parent OVOC being investigated; NO; and air (or O_2/N_2 mixtures). Production of the nitrates of direct interest here and other oxygenated products, as well as the loss of the parent OVOC, is followed quantitatively using an array of analytical techniques, described in more detail below. Collaborative work involving analysis of NCAR chamber samples using GC-ITMS instrumentation was also conducted.

Methods used at CU-Boulder (Ziemann laboratory)

The chamber at the University of Colorado was used to carry out a detailed study of the OH-initiated oxidation of di-n-octyl ether ($nC_8H_{17}\text{-O-n-}C_8H_{17}$, hereafter dioctyl ether). Experimental procedures are described here in a somewhat abbreviated form; full details are provided in (Ziola et al., in preparation, 2025).

Briefly, the experiments were conducted at room temperature (24°C) and atmospheric pressure (0.83 atm) in a 6.5 m^3 FEP Teflon chamber with blacklights installed on two walls. The chamber was filled with the following components, with mixing of chamber contents using a Teflon-coated fan:

1) Clean and dry air (<5 ppb hydrocarbons, <0.1% RH), from an Aadco pure air generator (near 1 atm total pressure).
2) Decane (1.0 ppm, used as a reference for later gas-phase analysis) and dioctyl ether (the precursor under investigation, 1.0 ppm), from a vaporizer system previously described [Finewax et al.[31]]
3) NO and isopropyl nitrite (the photolytic source of OH), each at 5 ppm.
4) 140 $\mu g\ m^{-3}$ of dioctyl phthalate (DOP) aerosol seed particles, via injection of an 11 $mg\ mL^{-1}$ DOP/acetonitrile solution.

The blacklights (which provide a sunlight surrogate) were turned on for 120 s, which led to photolysis of the isopropyl nitrite and formation of OH radicals, which then initiated the oxidation of the DOE and led to formation of a vast array of partially oxidized products:

$$CH_3CH(CH_3)ONO + h\nu \rightarrow CH_3CH(CH_3)O\bullet + NO$$
$$CH_3CH(CH_3)O\bullet + O_2 \rightarrow CH_3C(=O)CH_3 + HO_2$$
$$HO_2 + NO \rightarrow OH + NO_2$$
$$OH + \text{Dioctyl Ether} \rightarrow\rightarrow\rightarrow\rightarrow \text{Products}$$

Sampling of the gas phase chamber contents (before and after the photolysis period) was conducted by flowing chamber air through Tenax adsorbent tubes for later offline analysis. In addition, organic aerosol (OA) particles, composed of secondary organic aerosol (SOA) formed in the dioctyl ether oxidation and the DOP seed were collected onto pre-weighed Fluoropore 0.45 µm PTFE Membrane Millipore filters in two samplers operating in parallel. The Tenax cartridge samples were analyzed for gas phase constituents using a combination GC-FID / GC-ITMS instrument, while the filter samples were analyzed using an array of techniques, including GC-FID / GC-ITMS, Attenuated Total Reflectance FTIR (ATR-FTIR), HPLC–UV absorption, and I^--CIMS.

Throughout the experiment, a Thermo Environmental Instruments 42D NO-NO_2-NO_x analyzer continuously measured NO and NO_x concentrations and a scanning mobility particle sizer (SMPS) measured the OA volume distribution.

The NCAR Chamber

Studies at NCAR were conducted in a stainless steel, temperature-controlled environmental reaction chamber. The chamber is 2 m long, and has a volume of 47 l. Gases are added to the chamber using a glass vacuum line using standard manometric techniques. Oxidation is initiated by reaction with Cl-atoms, which were generated in the chamber by Cl_2 photolysis.

$$Cl_2 + h\nu \rightarrow Cl + Cl$$
$$Cl + VOC \rightarrow \text{products}$$

Infrared spectra of the starting materials and products are measured using a Bomem DA-8 FTIR spectrometer. The chamber is interfaced to the FTIR via a set of Hanst-type multi-pass optics that allow for 32 m of absorption path. Between 200 and 400 scans are typically averaged to improve the signal to noise. Concentrations are obtained by spectral subtraction (stripping) of the spectrum of a pure standard when available, or using cross sections obtained from the literature. Calibrated spectra for the multifunctional nitrates being quantified here are not available, hence cross sections typical of alkyl nitrates are used for quantification. Nitrate absorption bands are located near 1280 cm^{-1} and 1650 cm^{-1}, with integrated band strengths of 3.0 x 10^{-17} cm^{2} molec^{-1} and 5.4 x 10^{-17} cm^{2} molec^{-1}, respectively.

Compounds in the chamber are also identified and quantified using an Agilent 6890N gas chromatograph equipped with a flame ionization detector (FID) [McGillen et al., 2016]. Gas is flowed from the chamber through a 1/8" o.d. tube to a 6-port valve. Samples are collected in a 25 cm long loop of 1.6-mm o.d. PEEK tubing at ambient temperature connected to the 6-port valve, before injection into the GC. The GC temperature profile is 3 minutes at 28 ^{o}C, followed by a ramp of 20 ^{o}C min^{-1} for 7.1 minutes, to bring the temperature to 170 ^{o}C, followed by 1 minute at 170 ^{o}C.

Generally, for the types of compounds investigated here, nitrates are found to elute from this particular column setup about 5 min after their precursor, as shown in Figure 1 below. Clearly, there is rather close correspondence between the positioning of species like n-pentane and diethyl ether and the positioning of their nitrate derivatives, reflecting the similar vapor pressures of these species and providing a convenient method for identification of the nitrates of interest. Quantification of the nitrates in the GC was done using effective carbon number, which was assumed to be 0.5 less than the parent OVOC; this estimate is likely accurate to ±25%. Overall, the nitrate yields identified here were found to be quite small and thus subject to additional uncertainties due to weak signal levels (both FTIR and GC-FID). The GC-FID data are regarded as more reliable, as individual peaks can be directly attributed to nitrates of interest, while FTIR observations cannot distinguish individual nitrates. Overall, uncertainties in nitrate quantification are likely in the ± (35-50)% range in most cases, and possibly larger when yields are vanishingly small.

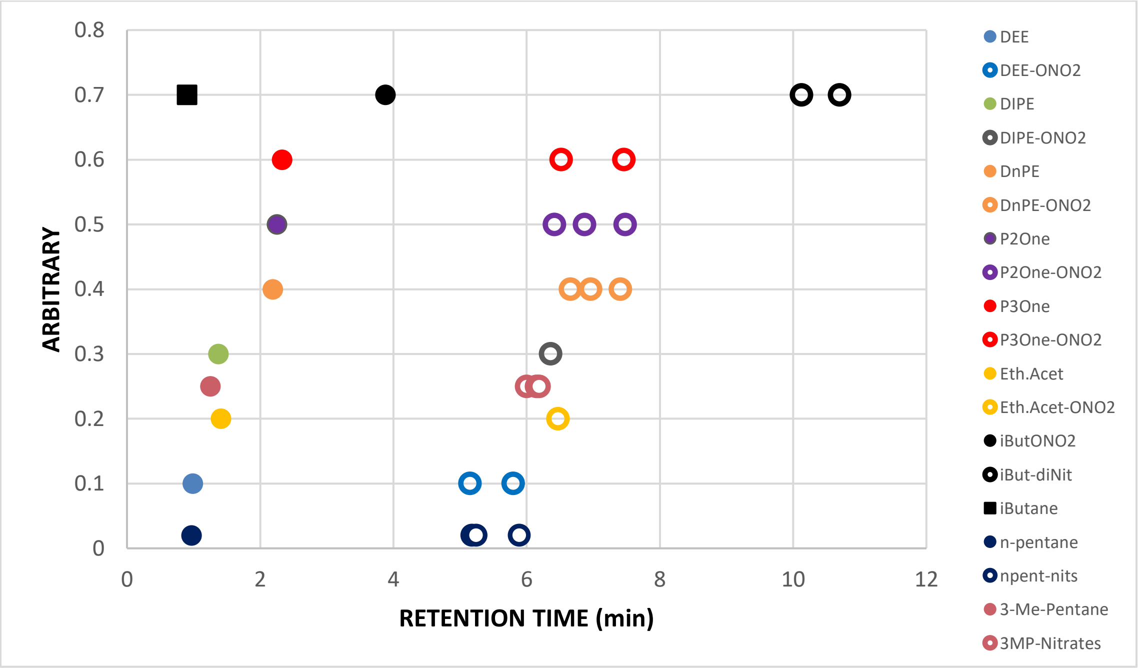

Figure 1: GC-FID retention time for many of the molecules of interest in this study (as well as for some alkanes) and their nitrate derivatives. Filled symbols, parent (O)VOC; open symbols, corresponding nitrate. Black: isobutane, isobutyl nitrate, isobutyl dinitrates (tentative). Red: 3-pentanone. Purple: 2-pentanone. Green: di-n-propyl ether. Grey: di-isopropyl ether. Orange: 3-methyl pentane. Yellow: ethyl acetate. Light blue: diethyl ether. Dark blue: n-pentane.

Use of GC-ITMS at CU for analysis of NCAR Chamber Samples

Another method used to aid in the identification of functionalized nitrates formed at NCAR was to sample photolyzed NCAR chamber contents onto Tenax and run these samples through the CU GC-ITMS instrument. To accomplish this, a non-polar GC column (identical to that used at NCAR) was installed at CU. In this way, elution times from the two columns are directly correlated (despite differences in flow rates and temperature profiles used in the two systems). The calibration curve (consisting of observations of CU retention time vs NCAR retention time for six species) is shown in Figure 2 below.

Once this correlation was established, the next step was to conduct 'typical' experiments (as described elsewhere in this report) in the NCAR stainless steel chamber, photolyzing $Cl_2/OVOC/NO/O_2/N_2$ mixtures and analyzing pre- and post-photolyzed mixtures via FT-IR and GC-FID. Simultaneously, samples were collected from the chamber onto Tenax cartridges before and after photolysis, and run through the GC-ITMS instrument at CU. Experiments of this nature were conducted on many of the OVOCs studied at NCAR, and in some cases, this type of analysis was helpful in confirming that peaks identified as nitrates at NCAR (typically at 5-7 min retention time) were indeed nitrates (9-13 min retention time, and m/z 46 peak due to NO_2^+).

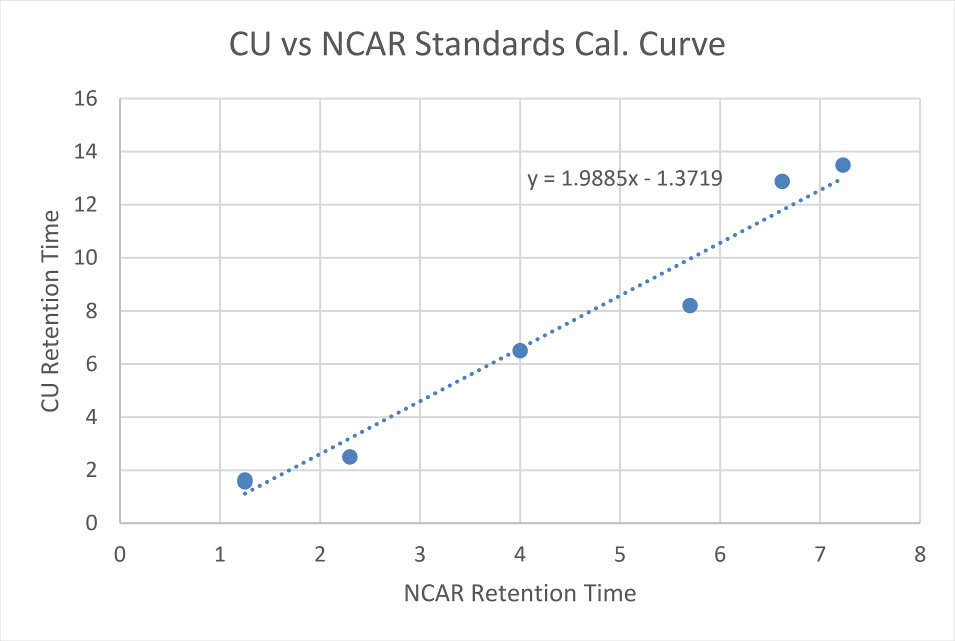

Figure 2: Comparison of retention times from the CU GC-ITMS and the NCAR GC-FID for a set of six organic species.

OBSERVATIONS

Dioctyl Ether at CU

This molecule, $nC_8H_{17}\text{-O-n-}C_8H_{17}$, was the subject of a detailed study conducted in the CU-Boulder chamber, using the full array of analytical tools described above. A full quantification of the reaction products formed in the oxidation of this species, formed in both the gas- and condensed phase, was achieved as summarized in the reaction mechanisms shown below and in Table 1.

a) Reaction Mechanism

The reaction mechanism, including branching ratios to various pathways, is summarized in the reaction schemes below. Yields of various compounds detected are summarized in the table, and account in full (within experimental uncertainty) for the oxidative processes occurring. The mechanism is based on that of an alkane of similar size, but with substantial modifications (based on our observations) that are induced by the presence of the ether functionality.

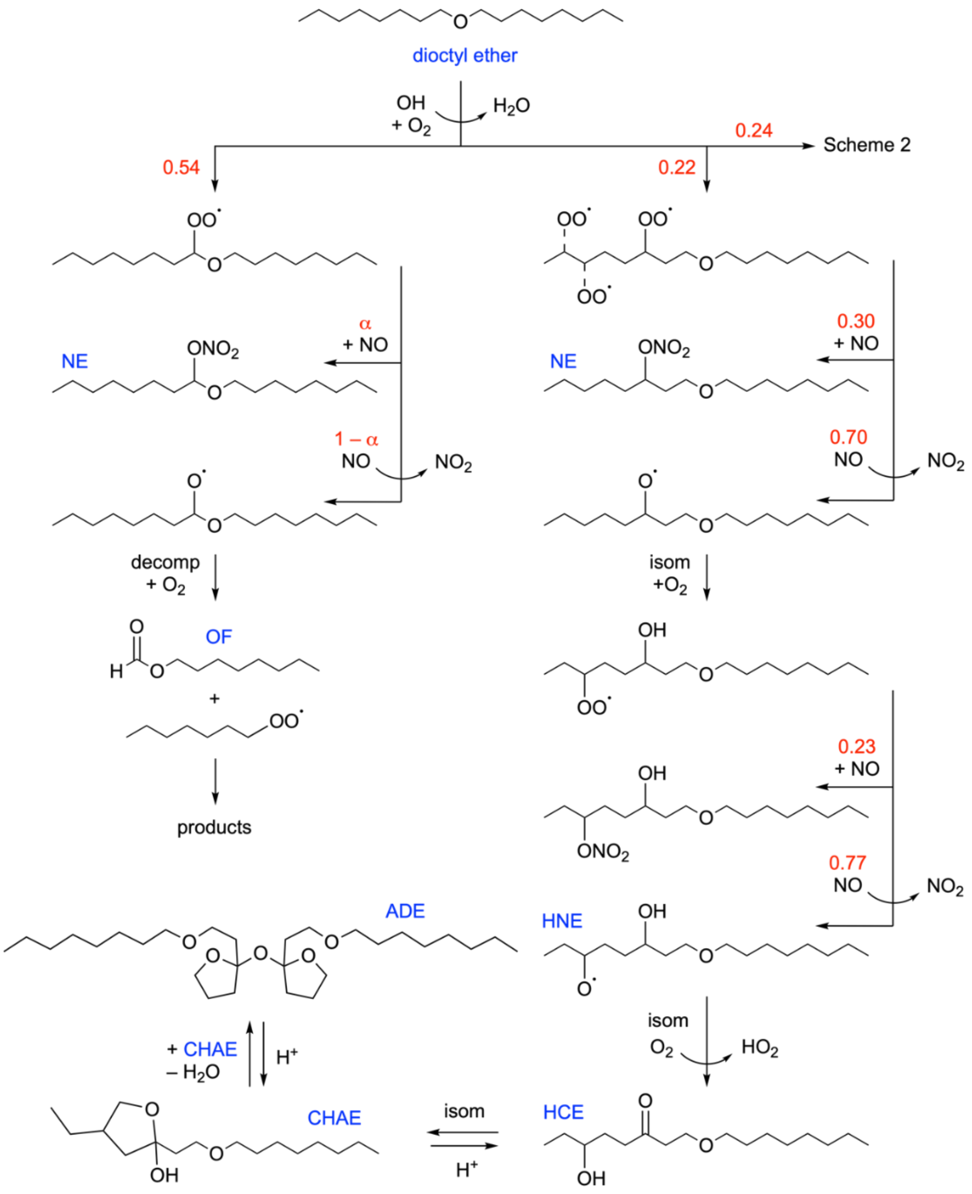

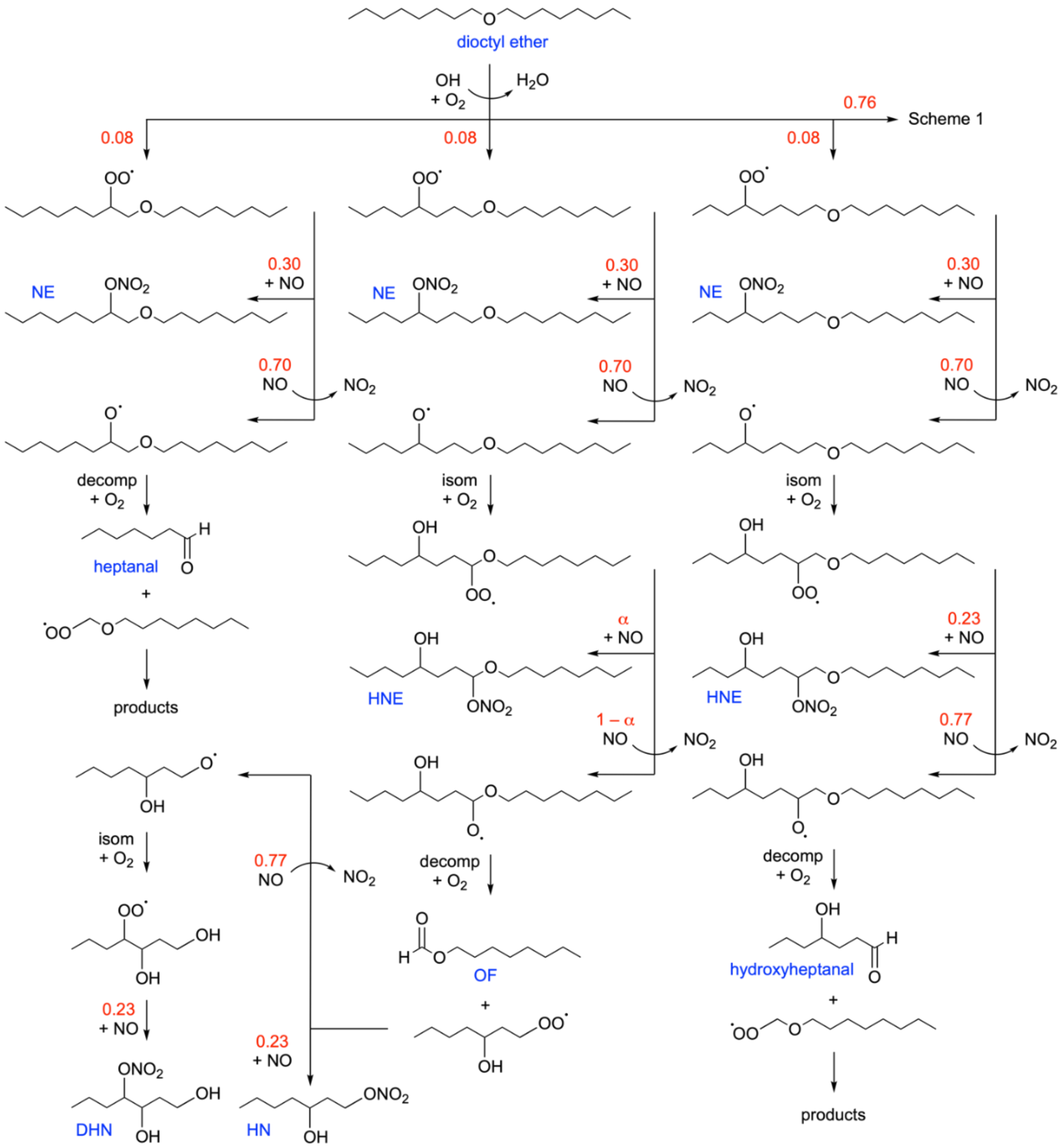

Scheme 1. Mechanism of gas-phase reaction of octyl ether with OH/NO_x.

A summary of key findings is given here:

1) The overall nitrate ether (NE) yield for octyl ether is found to be 15%, which is roughly half that of the ≈30% nitrate yield found for an alkane of similar size (e.g., hexadecane, $C_{16}H_{34}$). ***The reduced overall nitrate yield means that more local ozone production will occur when a large ether of this sort is oxidized in an urban region compared to a comparably sized alkane.***

2) The reason for this difference in nitrate yield appears to be due to a very much reduced nitrate formation yield in the reaction of NO with the major peroxy radical formed in the system, that formed following OH attack at C_1, the carbon atom adjacent to the ether. This chemistry is shown at the top left of Scheme 1, with the analysis leading to a value of α (and hence a nitrate yield) of 0.08. As alluded to above, this branching to nitrate formation of 0.08 is very different from the 0.30 expected for an alkane.

3) As determined using GC-FID, a major gas-phase product of the chemistry is octyl formate (nC_8H_{17}-O-CH=O), see Figure 3. This species is observed with a yield of 55%, and is the expected product of the chemistry occurring following OH attack at C_1 (see again the top left of Scheme 1). Given that roughly 57% of the OH attack on dioctyl ether is expected to occur at C_1 (based on structure-reactivity relationships) and that there are additional minor octyl formate production channels in the chemistry), the observations of high octyl formate yield (55%) and low nitrate yield from this channel (8%) are internally consistent.

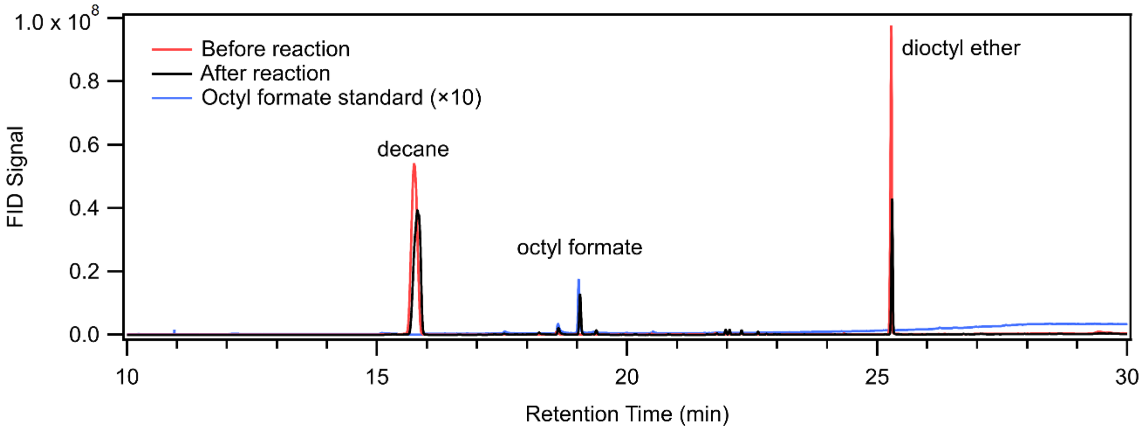

Figure 3. Overlaid GC-FID chromatograms of decane and dioctyl ether reactants and octyl formate product collected in Tenax adsorbent tubes before and after the dioctyl ether + OH/NO_x reaction, and an octyl formate standard added to the chamber in a separate experiment.

4) As was already described, SOA formed during dioctyl ether oxidation were collected on filters and analyzed using various techniques. Among the classes of species found in the SOA are the nitrate ethers (Point 1 above) and hydroxynitrate ethers, both detected by HPLC with UV detection (at 210 nm, where nitrates absorb strongly) – see Figure 4. In a broader sense, ***the presence of the ether linkage lowers the SOA formation yield compared to an alkane of comparable size***. This is due to a greater propensity for decomposition of alkoxy radicals where the radical center is located near to the ether functionality. The formation of octyl formate noted above (nine carbons rather than 16) with a yield of 55% is the primary example of this enhanced propensity for decomposition.

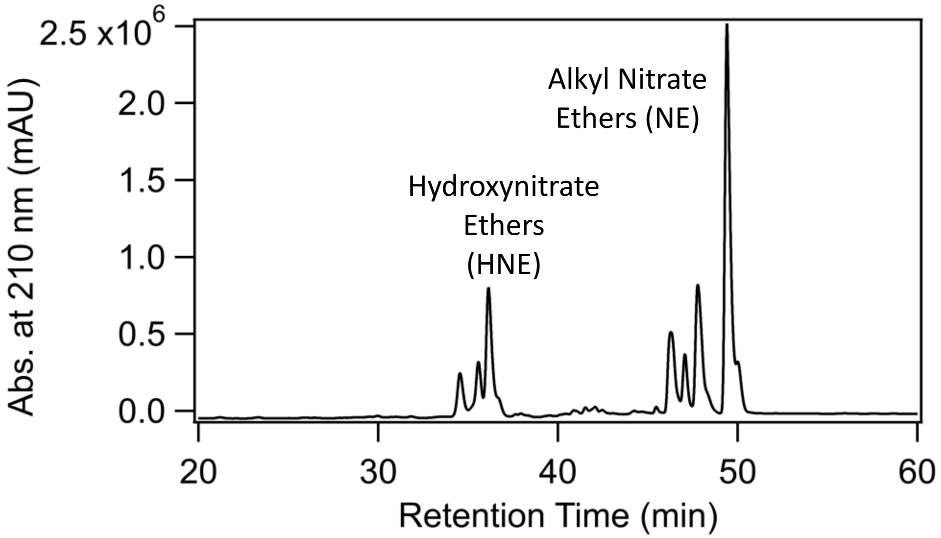

Figure 4. HPLC chromatogram of SOA formed from the reaction of dioctyl ether with OH/NO_x.

5) Overall, and rather remarkably, the presence of the ether group in dioctyl ether leads to a modification of about 78% of the chemistry relative to what is found for an alkane of similar size, despite the fact that this ether oxygen atom makes up only ≈6% of the molecule (e.g., compare heptadecane [$C_{17}H_{36}$] with dioctyl ether [$C_{16}H_{34}O$]).

Table 1. Modeled and Measured Molar Yields of Dioctyl Ether + OH/NO_x Reaction Products. See the reaction schemes for the origins of the products listed.

Product	Model Yield Equation	Molar Yield	
		Modeled	Measured
OF (Octyl formate)	$[0.54 \times (1-\alpha)] + [0.08 \times 0.70 \times (1-\alpha)]$	0.55	0.55
NE (nitrate ethers)	$[0.54 \times \alpha] + [0.22 \times 0.30]$ $+ 3 \times ([0.08 \times 0.30])$	0.18	0.15
HNE (hydroxy-nitrate ethers)	$[0.22 \times 0.70 \times 0.23] + [0.08 \times 0.70 \times \alpha]$ $+ [0.08 \times 0.70 \times 0.23]$	0.05	0.05
HCE, CHAE, ADE	$[0.22 \times 0.70 \times 0.77]$	0.12	0.19
HC (hydroxy-carbonyls)	$[0.54 \times (1-\alpha) \times 0.79 \times 0.82]$ $+ [0.08 \times 0.70 \times 0.77]$	0.36	ND[a]
Heptanal	$[0.08 \times 0.70]$ $+ [0.08 \times 0.70 \times (1-\alpha) \times 0.78]$ $+ [0.08 \times 0.70 \times 0.77 \times (1-\alpha) \times 0.78]$	0.13	ND
AN (alkyl nitrates)	$[0.54 \times (1-\alpha) \times 0.21]$	0.10	ND
HN (hydroxy-nitrates)	$[0.54 \times (1-\alpha) \times 0.79 \times 0.18]$	0.07	ND
DHN (dihydroxy-nitrates)	$[0.08 \times \times 0.70 \times (1-\alpha) \times 0.80 \times 0.21]$	0.01	DNQ[b]
EN (ether nitrate)	$[0.08 \times 0.70 \times \alpha]$ $+ [0.08 \times 0.70 \times 0.77 \times \alpha]$	0.01	ND
HEN (hydroxyether nitrates)	$[0.08 \times \times 0.70 \times (1-\alpha) \times 0.22]$ $[0.08 \times \times 0.70 \times 0.77 \times (1-\alpha) \times 0.22]$	0.02	ND

** Hydrocarbonyl ethers (HCE), Cyclic hemiacetal ethers (CHAE), Acetal Dimer Ethers (ADE)

[a] Not detected. [b] Detected but not quantified

Studies of smaller molecules at NCAR

The goal of the NCAR portion of the study was to determine the yield of organic nitrates formed in the oxidation of oxygenated organics, including ethers, esters, ketones and multifunctional species containing 5-8 heavy atoms (C,O). As discussed in the introduction, the organic nitrates and ozone are anti-correlated, as NO_2 photolysis generates ozone.

$$OH + RH\ (+ O_2) \rightarrow RO_2 + H_2O$$

$$RO_2 + NO \rightarrow RO + NO_2 \qquad \text{(major channel, branching ratio } 1\text{-}\alpha\text{)}$$

$$RO_2 + NO + M \rightarrow RONO_2 + M \qquad \text{(minor channel, branching ratio } \alpha\text{)}$$

For most studies described here, Cl-atoms are used in place of OH for simplicity and has no impact on the findings. A large number of molecules were studied, to admittedly varying degrees of detail but, as will be seen, yields of nitrates are small in all cases studied.

n-Pentane, $CH_3CH_2CH_2CH_2CH_3$

As a primer, a summary of a study of n-pentane ($CH_3CH_2CH_2CH_2CH_3$) conducted in the NCAR chamber (supported by a previous CRC grant) is given here for comparison with results from the more complex oxygenated species that follow.

Because OH can abstract an H-atom from three unique sites in n-pentane (the central CH_2 group; either of the two identical CH_2 groups adjacent to the central CH_2; and the CH_3 group), three distinct peroxy radical species can be formed and their subsequent reactions with NO can then generate three distinct organic nitrates: 3-pentyl nitrate, ($CH_3CH_2CH(ONO_2)CH_2CH_3$); 2-pentyl nitrate ($CH_3CH_2CH_2CH(ONO_2)CH_3$) and 1-pentyl nitrate ($CH_3CH_2CH_2CH_2CH_2ONO_2$). Three nitrates were indeed observed in the experiments, as expected. Relative to the loss of n-pentane (as determined by FTIR), the yields of the three nitrates were found to be 0.047, 0.065, and 0.011, respectively, leading to a total nitrate yield of 12% - see Table 2 for a summary. Similar experiments on hexanes showed total nitrate yields of about 17%. As these C5-C6 species are of similar size to the molecules reported upon herein, they serve as useful comparators for the data about to be presented. Diethyl ether ($CH_3CH_2OCH_2CH_3$) and dimethoxy methane ($CH_3OCH_2OCH_3$) bear strong similarities to n-pentane and hence comparisons between these species are particularly informative.

	1-Pentyl Nitrate (Primary)	**2-Pentyl Nitrate (Secondary)**	**3-Pentyl Nitrate (Secondary)**
Site of Attack (%)	9 %	54 %	37 %
Measured Yield (%)	1.1	6.5	4.7
Normalized Yield (per RO_2 formed)	**0.11**	**0.12**	**0.13**

Table 2: Summary of nitrate yields from n-pentane (Tyndall et al., in preparation, 2025)

Diethyl Ether

The reaction of Cl-atoms with diethyl ether proceeds to a very large degree by abstraction at the $-CH_2-$ positions of the molecule. Thus, in the presence of oxygen, near-quantitative production of the $CH_3CH_2OCH(OO\bullet)CH_3$ peroxy radical is expected:

$$Cl_2 \rightarrow Cl + Cl$$
$$Cl + CH_3CH_2OCH_2CH_3 \rightarrow CH_3CH_2OCH\bullet CH_3 + HCl$$
$$CH_3CH_2OCH\bullet CH_3 + O_2 \rightarrow CH_3CH_2OCH(OO\bullet)CH_3$$

Subsequent reaction of this radical with NO will generate the alkoxy species $CH_3CH_2OCH(O\bullet)CH_3$ in large yield (with NO_2 as a co-product), and (possibly) the organic nitrate of specific interest in this study, $CH_3CH_2OCH(ONO_2)CH_3$. Previous studies conducted in our laboratory (and confirmed here) show that two pathways are available to the $CH_3CH_2OCH(O\bullet)CH_3$ radical, reaction with O_2 and decomposition. The chemistry is complex but can be summarized as follows, with major end-products being ethyl formate ($CH_3CH_2OCH{=}O$) and ethyl acetate ($CH_3CH_2OC({=}O)CH_3$):

$$CH_3CH_2OCH(OO\bullet)CH_3 + NO \rightarrow [CH_3CH_2OCH(O\bullet)CH_3]^* + NO_2$$

$$CH_3CH_2OCH(OO\bullet)CH_3 + NO \rightarrow CH_3CH_2OCH(ONO_2)CH_3$$
$$[CH_3CH_2OCH(O\bullet)CH_3]^* \rightarrow CH_3CH_2OCH(O\bullet)CH_3$$
$$CH_3CH_2OCH(O\bullet)CH_3 + O_2 \rightarrow \mathbf{CH_3CH_2OC(=O)CH_3} + HO_2$$
$$CH_3CH_2OCH(O\bullet)CH_3 \rightarrow \mathbf{CH_3CH_2OCH{=}O} + \bullet CH_3$$

Ethyl formate and ethyl acetate are indeed observed via FTIR spectroscopy (as shown in Figure 5) and via GC-FID analysis, with yields of approx. 64% and 10% respectively, in the presence of NO and 1 atm of air. Methyl nitrate is also a by-product of the chemistry and is observed via both FTIR and GC-FID.

$$\bullet CH_3 + O_2 \rightarrow CH_3OO\bullet$$
$$CH_3OO\bullet + NO \rightarrow CH_3O\bullet + NO_2$$
$$CH_3O\bullet + NO_2 \rightarrow CH_3ONO_2$$

After subtraction of the methyl nitrate FTIR absorption features, only weak absorption features remain in the nitrate regions of the spectrum (near 1280 and 1660 cm^{-1}). Attributing all of this remaining absorption to the DEE-derived nitrates leads to an overall nitrate yield of 2 ± 2%. Analysis of GC-FID data obtained in diethyl ether oxidation shows two peaks (located between 5 and 6 minutes elution time, see Figure 6) that elute at nearly identical times to 2-pentyl nitrate and 1-pentyl nitrate and thus are almost assuredly due to the DEE-derived nitrates, $CH_3CH_2OCH(ONO_2)CH_3$ and $CH_3CH_2OCH_2CH_2ONO_2$. Collectively, their yield is quite small, roughly 1±1% when summed together, consistent with the 2±2% yield estimated via FTIR. Of particular note is that in a couple of experiments, 2-3 GC analyses were done consecutively on a previously-photolyzed chamber mixture, a process that takes up to 75 min. Repeated samples showed no change – i.e., the concentration of the ether-derived organic nitrates did not decrease over the time period required to conduct the multiple GC runs, indicating no significant wall loss was occurring in the chamber. Of particular interest is the apparent low yield of $CH_3CH_2OCH(ONO_2)CH_3$ (the first of the two peaks shown), despite the high yield of its precursor peroxy radical, indicating the likelihood that the ether group is suppressing nitrate formation at the adjacent site, as was also found with dioctyl ether above.

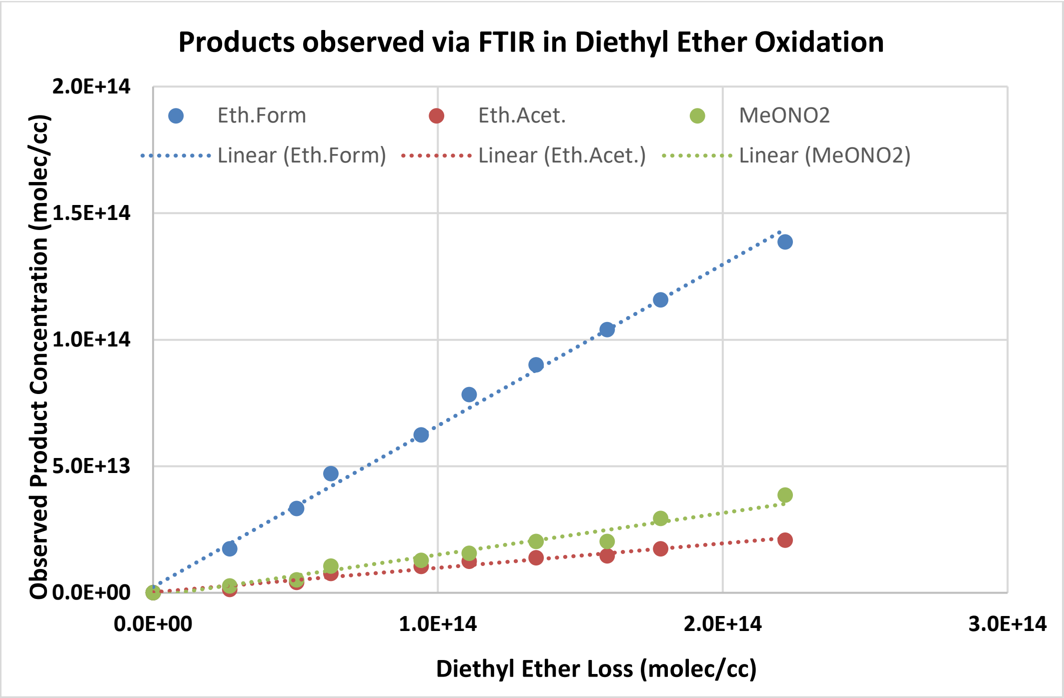

Figure 5: Observed concentrations of ethyl formate, ethyl acetate and methyl nitrate from the Cl-atom initiated oxidation of diethyl ether.

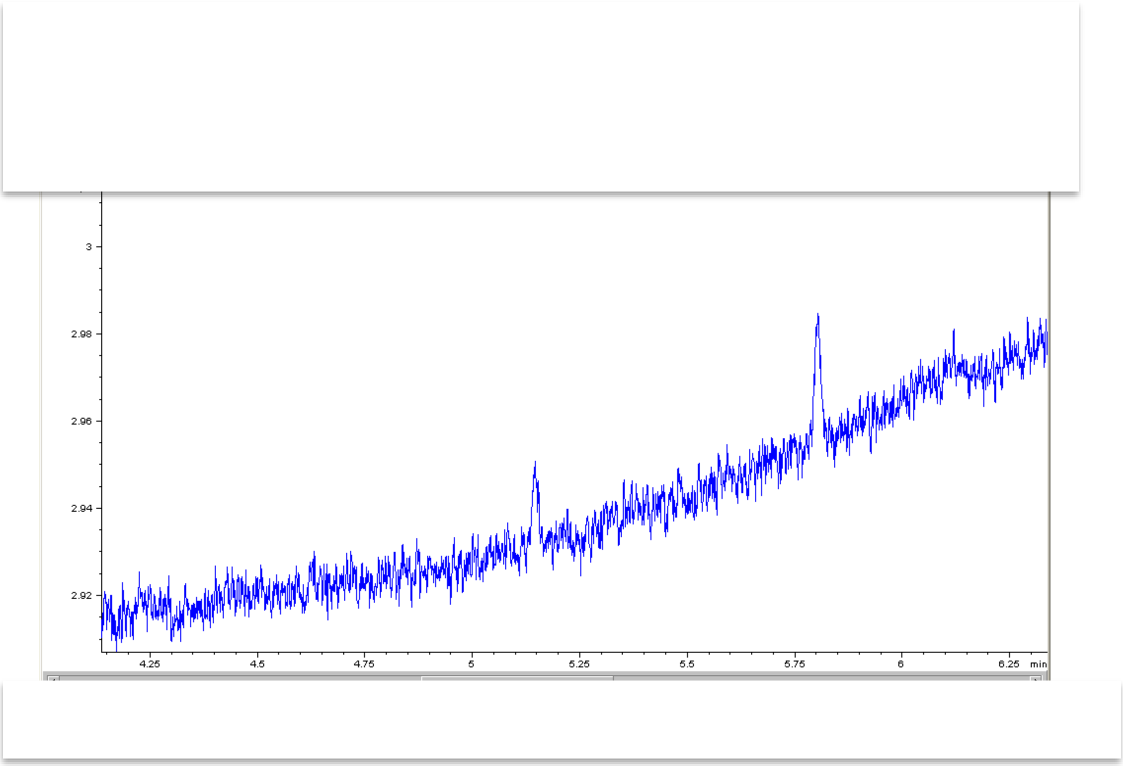

Figure 6: A portion of the GC-FID spectrum obtained following irradiation of Cl2/diethyl ether/ NO/O2/N2 mixtures in the NCAR chamber, tentatively showing the formation of two nitrate species.

Dimethoxy-methane (DMM, CH_3O-CH_2-OCH_3)

As with n-pentane and DEE, DMM possesses five heavy atoms and in this case only C-O single bonds. Not surprisingly then, its vapor pressure, and hence elution time from the GC-FID column (1.0

min), is very similar to that of n-pentane and DEE, and nitrate by-products are then likely to appear at similar retention times to those of the n-pentane and DEE (5-6 min). Photolysis of Cl_2/DMM/NO/O_2/N_2 mixtures were conducted in the NCAR chamber. Reaction of Cl-atoms with DMM can occur at two unique sites, generating (in the presence of O_2) two peroxy radicals:

$$Cl + CH_3O\text{-}CH_2\text{-}OCH_3 \rightarrow CH_3O\text{-}CH(OO\bullet)\text{-}OCH_3 \quad (a)$$

$$Cl + CH_3O\text{-}CH_2\text{-}OCH_3 \rightarrow CH_3O\text{-}CH_2\text{-}OCH_2(OO\bullet) \quad (b)$$

Studies by Wallington et al. indicated that 75% of the Cl/DMM reaction occurs via pathway (b), while 25% occurs via (a). Subsequent reactions of the peroxy radicals, in addition to generating NO_2 and the alkoxy species, could lead to two nitrates, highlighted below:

$$CH_3O\text{-}CH(OO\bullet)\text{-}OCH_3 + NO \rightarrow \mathbf{CH_3O\text{-}CH(ONO_2)\text{-}OCH_3} \quad (a)$$

$$CH_3O\text{-}CH_2\text{-}OCH_2(OO\bullet) + NO \rightarrow \mathbf{CH_3O\text{-}CH_2\text{-}OCH_2(ONO_2}) \quad (b)$$

The two alkoxy radicals formed subsequently lead to dimethyl carbonate, $CH_3O\text{-}C(=O)\text{-}OCH_3$, and a formate ester ($CH_3O\text{-}CH_2\text{-}OCHO$) in yields of roughly 25 and 75% respectively. (Wallington et al., 1997). From comparisons of IR spectra presented in that paper and those obtained herein, both of these products were formed in our experiment (although we do not yet have authentic samples to allow quantification). Two GC-FID peaks near 1.5 and 1.6 min likely correspond to these species.

With respect to nitrate production, the infrared spectra showed some evidence for typical nitrate absorption bands at 1670 but the band near 1280 is obscured by the carbonate product; a rough IR-derived nitrate yield of 2% is obtained. The GC-FID chromatograms did show one quantifiable nitrate peak (5.2 min), at an elution time nearly identical to those for 2- and 3-pentyl nitrate as well as the DEE-derived nitrate. With reasonable assumptions about the GC sensitivity of this compound relative to that of DMM, a nitrate yield of 4±2% is obtained (relative to DMM consumption), broadly consistent with the IR observations. As with DEE above, repeat measurements of chamber contents via GC-FID showed that little wall loss of the nitrate was occurring. Which specific nitrate (or nitrates) this peak corresponds to is unknown.

Di-isopropyl ether (DIPE)

A brief study was carried out in the NCAR chamber on the Cl-atom initiated oxidation of di-isopropyl ether (DIPE), $CH_3CH(CH_3)\text{-}O\text{-}CH(CH_3)CH_3$, in the presence of NOx. The majority of the chemistry is expected to occur via reaction of Cl at the tertiary –CH< groups, leading to the formation of $CH_3CH(CH_3)\text{-}O\text{-}C(=O)CH_3$, with CH_3ONO_2 as a minor co-product of this chemistry. These species are clearly observed in the FTIR. After accounting for the presence of methyl nitrate in the FTIR spectra obtained, very little residual absorption is present near 1280 or 1660 cm^{-1}, and a nitrate yields of about 3±2% is obtained. GC-FID chromatograms show a peak at 6.36 min, that is likely attributable to the nitrate of interest, $CH_3CH(CH_3)\text{-}O\text{-}C(ONO_2)(CH_3)CH_3$. (No other peaks are present in this part of the chromatogram). With reasonable assumptions about the GC sensitivity of this compound relative to that of DIPE, a yield of 4±2% is obtained, consistent with the FTIR results. This yield is considerably smaller than that obtained from methyl-substituted pentanes (e.g., a nitrate yield of 18% was obtained in our previous studies of 2,4-dimethylpentane), again indicating the likelihood of suppression of nitrate formation by the presence of the ether functionality.

Di-n-propyl ether

A cursorial study of the Cl-atom initiated oxidation of di-n-propyl ether (DnPE) was conducted at NCAR. Experiments should be regarded as preliminary at this point, as full calibration of product yields using authentic samples has not yet been carried out. Experiments have been conducted with and without NOx added to the system. The reaction of Cl-atoms (or OH radicals, which are also formed in NO is present) with di-n-propyl ether (DnPE) is expected to mainly (but not exclusively) occur at the carbon closest to the ether linkage:

$$\mathrm{Cl + CH_3CH_2CH_2OCH_2CH_2CH_3\ (+\ O_2) \rightarrow HCl + CH_3CH_2CH_2OCH(OO\bullet)CH_2CH_3}$$

In the presence of NOx, the formation of n-propyl formate (nPF) and acetaldehyde (CH_3CHO) would be expected from the ensuing chemistry of this radical [Semples et al., 2000]:

$$\mathrm{CH_3CH_2CH_2OCH(OO\bullet)CH_2CH_3 + NO \rightarrow CH_3CH_2CH_2OCH(O\bullet)CH_2CH_3 + NO_2}$$
$$\mathrm{CH_3CH_2CH_2OCH(O\bullet)CH_2CH_3 \rightarrow CH_3CH_2CH_2OCH{=}O\ (nPF) + CH_3CH_2}$$
$$\mathrm{CH_3CH_2 \rightarrow\rightarrow\rightarrow CH_3CHO,\ CH_3CH_2ONO_2}$$

Examination of GC-FID chromatograms obtained following photolysis of Cl_2/DnPE/NO/O_2/N_2 mixtures, with NO and DnPE both present at levels of 25-45 ppm, clearly showed evidence for acetaldehyde formation (0.83 min retention time). While we do not yet have an authentic sample of nPF for comparison, a major peak at 1.53 min is consistent with its expected retention time and is very likely due to this species. FTIR spectra also show spectral features very similar to ethyl formate (for which we do have calibrated spectra), again consistent with nPF formation in significant yields. Acetaldehyde is difficult to identify/quantify in the IR due to its weak absorption features, but evidence for its formation is also seen. Numerous additional peaks are seen with retention times of 4-6 min in the GC-FID spectra, consistent with the presence of reasonably low vapor pressure products, likely multi-functional in nature. These compounds will be difficult to identify and quantify however, due to a lack of authentic standards.

Of particular interest is observation of peaks in the infrared (centered at 1285 and 1660 cm^{-1}) that are almost assuredly due to organic nitrates. Use of standard IR absorption band strengths for organic nitrates implies a total yield of (8±3)% for these species relative to the loss of DnPE. At this point, the identity of these species cannot be established. Ethyl nitrate is an expected product of this system (via chemistry of the CH_3CH_2 co-product of nPF formation) and appears to contribute somewhat (though far from quantitatively) to the overall observed IR signal.

With respect to GC-FID analysis, five peaks are observed in the 6 - 7.5 min part of the chromatogram, three of which are likely due to the nitrates potentially formed from DnPE oxidation (although which three is at this point unknown). To obtain at least a rough estimate of the nitrate yield from analysis of these data, the area of all five peaks were summed to give a ballpark estimate of the nitrate yield. With reasonable assumptions regarding the GC sensitivity for the nitrates, a yield of about 3% is obtained.

Some DnPE oxidation experiments were also conducted in the absence of NOx, to provide complementary mechanistic information and to aid in product identification. As with the NOx-containing experiments, acetaldehyde was present, along with nPF, as significant products. A different array of GC-FID peaks were observed in the 4-7 min retention time window, and are likely the result of the various RO_2/HO_2 reactions that can occur in this complex system – again these peaks will be difficult to assign in the absence of authentic standards. However, none of the five peaks identified above as potential nitrates appeared in the absence of NO_x, which provides additional support for their identity as the nitrates of interest.

Ethyl Acetate

Experiments were also carried out at NCAR involving the photolysis of Cl_2/ethyl acetate/ $NO/O_2/N_2$ mixtures. While there are three sites from which H-atom abstraction can occur, the majority of the reaction (more than 75%, Orlando et al., 2010) occurs at the $-CH_2-$ group, with the ensuing chemistry given by the reactions below.

$$Cl + CH_3C(=O)OCH_2CH_3 \rightarrow CH_3C(=O)OCH\bullet CH_3 + HCl$$

$$CH_3C(=O)OCH\bullet CH_3 + O_2 \rightarrow CH_3C(=O)OCH(OO\bullet)CH_3$$

$$CH_3C(=O)OCH(OO\bullet)CH_3 + NO \rightarrow CH_3C(=O)OCH(O\bullet)CH_3 + NO_2$$

$$CH_3C(=O)OCH(O\bullet)CH_3 \rightarrow \mathbf{CH_3C(=O)OH} + CH_3C\bullet(=O)$$

$$CH_3C(=O)OCH(O\bullet)CH_3 + O_2 \rightarrow \mathbf{CH_3C(=O)OC(=O)CH_3} + HO_2$$

The formation of the major expected product in this chemistry, acetic acid ($CH_3C(=O)OH$), was confirmed via FTIR analysis. Also observed in small yield was acetic anhydride ($CH_3C(=O)OC(=O)CH_3$), with a yield that increased with increased O_2 partial pressure, as expected from the chemistry above. Methyl nitrate and PAN are also formed as minor products in this chemistry, as a by-product of $CH_3C(=O)$ production. After accounting for the presence of these nitrate-containing species in the FTIR spectra, some residual absorption near 1290 and 1680 cm^{-1} remained. If all is assumed to be nitrates, then the yield could be as high as 6±4%. But, this is almost assuredly an upper limit as peak positions and shapes do not exactly match those of typical nitrates, and there is considerably less absorption at 1290 cm^{-1} than at 1680 cm^{-1}, indicating the likely contribution of other species.

With regard to the GC-FID data, a peak located at 6.7 min is observed, consistent with the expected position of an ethyl acetate derived nitrate. The yield of this species, based on reasonable sensitivity is quite low, about 1±1%, and probably gives a more reliable indication of the actual nitrate yield.

There are two automated chemical mechanism generation software systems that are finding more and more use in the atmospheric chemistry community, GECKO-A (Aumont et al., 2005) and MechGen (Carter et al., 2024). These systems operate on a set of 'rules' that determine rates of chemical reactions for organic species under atmospheric conditions. As an interesting aside, we note that neither of these software systems predicts the chemistry of the $CH_3C(=O)OCH(O\bullet)CH_3$ radical particularly well. GECKO-A predicts CH_3 elimination to dominate, a pathway that has not been observed experimentally (to the best of our knowledge). MechGen does predict that acetic acid formation will dominate, but the predicted rate of this process is too fast (probably by roughly an order of magnitude) to allow for the formation of the minor amounts of acetic anhydride observed in this and other studies.

Although beyond the scope of this project, adjustment to the rules for determining rates of these ester-derived alkoxy species (based, for example, on already published ethyl acetate oxidation data) is warranted.

3-Pentanone

A set of experiments was conducted in the NCAR chamber to examine the products formed in the Cl-atom initiated oxidation of 3-pentanone in the presence of NOx. The majority (but not all) of the reaction of Cl with 3-pentanone is expected to occur at the -CH_2- groups:

$$Cl + CH_3CH_2C(=O)CH_2CH_3 \rightarrow CH_3CH_2C(=O)CH\bullet CH_3 + HCl$$
$$CH_3CH_2C(=O)CH\bullet CH_3 + O_2 \rightarrow CH_3CH_2C(=O)CH(OO\bullet)CH_3 + HCl$$
$$CH_3CH_2C(=O)CH(OO\bullet)CH_3 + NO \rightarrow CH_3CH_2C(=O)CH(O\bullet)CH_3 + NO_2$$
$$CH_3CH_2C(=O)CH(OO\bullet)CH_3 + NO \rightarrow CH_3CH_2C(=O)CH(ONO_2)CH_3$$
$$CH_3CH_2C(=O)CH(O\bullet)CH_3 \rightarrow CH_3CHO + CH_3CH_2C(=O)OO\bullet$$

Products clearly identified in the infrared following irradiation of Cl_2 / 3-pentanone / NO/ O_2 / N_2 mixtures are shown in Figure 7 from experiments conducted over a range of O_2 partial pressures (30-500 Torr). Products observed and quantified include PAN, PPN, acetaldehyde, formaldehyde and CO. These products are all consistent with expected chemistry following the decomposition of the $CH_3CH_2C(=O)CH(O\bullet)CH_3$ radical. Also observed in these experiments, but not shown in the figure, is CO_2. While CO_2 formation is expected, its yield appears to vary with the O_2 partial pressure – this chemistry is not currently understood, but likely results from chemistry occurring following Cl-atom attack at the CH_3 groups in 3-pentanone, leading to the formation of first the peroxy radical $CH_3CH_2C(=O)CH_2CH_2OO\bullet$ and then the alkoxy species $CH_3CH_2C(=O)CH_2CH_2O\bullet$. This subsequent chemistry involving these radical species is not quantitatively understood at present.

Organic nitrates appear to be present in the both the FTIR and GC-FID spectra. In the FTIR, formation of PAN, PPN and (particularly at low O2 partial pressures) ethyl nitrate make quantitative analysis difficult. Focusing predominantly on experiments conducted at high O_2 partial pressure (150 Torr and above), an overall (6±3)% organic nitrate yield is tentatively assigned, which could consist of either or both of the possible nitrate species $CH_3CH_2C(=O)CH(ONO_2)CH_3$, and $CH_3CH_2C(=O)CH_2CH_2ONO_2$. Note however that a contribution to this total from ethyl nitrate is also likely and the value given may be an overestimate.

Regarding the GC-FID analysis of nitrates from 3-pentanone oxidation, there is consistent evidence (from GC-ITMS, retention time, peak shape, experiments done with and without NOx, experiments involving NO_3 reaction with 2-pentene to provide an alternative path to generating the relevant nitrates) that peaks at 6.4 and 7.4 min are due to the nitrate species of interest, $CH_3CH_2C(=O)CH(ONO_2)CH_3$ and $CH_3CH_2C(=O)CH_2CH_2ONO_2$, respectively. With reasonable assumptions of GC-FID sensitivity, a yield of each species of about 1.5% is obtained (total nitrate yield $\approx 3 \pm 1.5\%$).

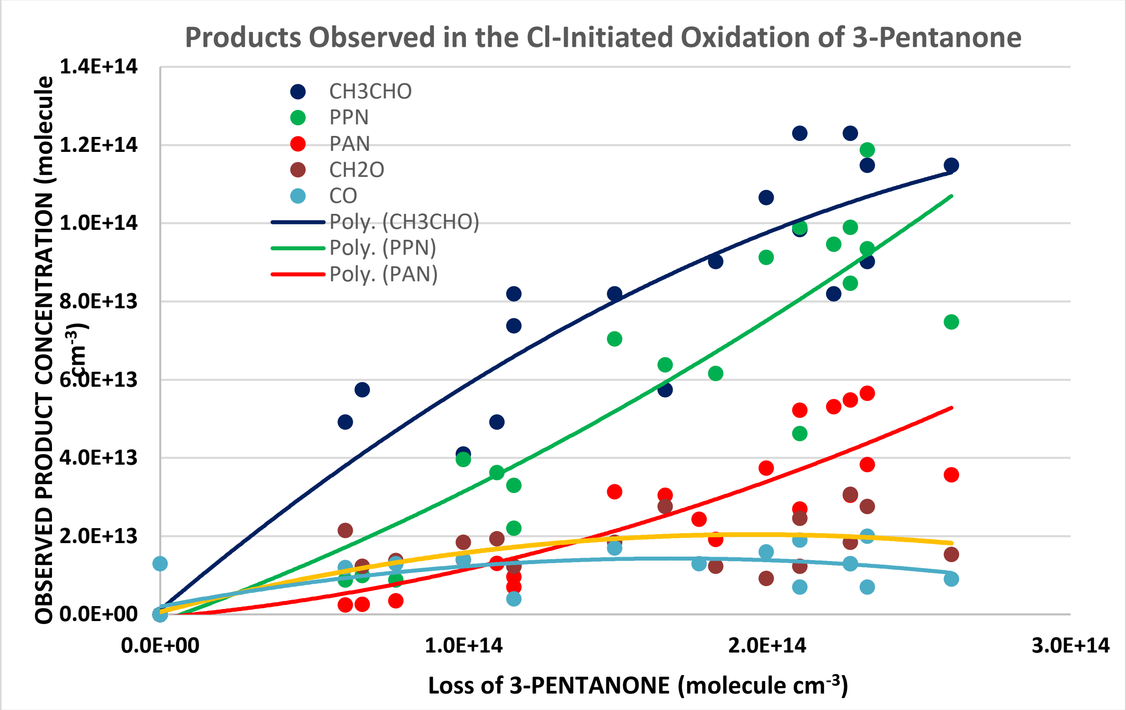

Figure 7: Observed concentrations of formed in the Cl-atom initiated oxidation of 3-pentanone in the presence of NO_x. All quantification is via infrared absorption.

2-Pentanone

Experiments were also conducted on 2-pentanone, $CH_3C(=O)CH_2CH_2CH_3$. The lack of symmetry in this molecule leads to complex chemistry; while four peroxy radicals are formed in total, focus will be on the two (in bold) likely to be formed in highest yield:

Cl/OH + $CH_3C(=O)CH_2CH_2CH_3$ → **$CH_3C(=O)CH(OO\bullet)CH_2CH_3$** + HCl/$H_2O$
→ **$CH_3C(=O)CH_2CH(OO\bullet)CH_3$** + HCl/$H_2O$

Products clearly identified and quantified include CO_2, PAN, propanal, CH_2O and organic nitrates, see Figure 8. Chemistry occurring subsequent to formation of $CH_3C(=O)CH(OO\bullet)CH_2CH_3$ is very likely to lead to the formation of propanal, with either PAN or (CO_2 and CH_2O) as co-products, entirely consistent with our observations. However, it appears that these species only account for about half of the 2-pentanone loss.

The products resulting following $CH_3C(=O)CH_2CH(OO\bullet)CH_3$ formation are less clear. One possible end-product is 2,4-pentadione, also known as acetyl acetone. It is interesting to note that this species is thought to exist in its enol form, i.e., $CH_3C(=O)CH=C(OH)CH_3$, rather than as the dione, making it quite reactive (Zhou et al., 2008); interestingly, comparison with a purchased standard has shown no evidence for the formation of this species (in the enol form) via GC-FID or FTIR. Other pathways for $CH_3C(=O)CH_2CH(OO\bullet)CH_3$ might result in acetaldehyde with multiple co-products (CH_2O, CO_2, and PAN) possible. As already stated, CH_2O, CO_2 and PAN are clearly observed and quantifiable, as is acetaldehyde (not yet quantified). As an aside, we note that the Leeds Master Chemical Mechanism (MCM, http://mcm.york.ac.uk/browse.htt?species=MPRK) predicts a very different chemistry pursuant to formation of this radical, involving alkoxy radical isomerization, chemistry that to us seems unlikely. On the other hand, the GECKO-A mechanism generation system, http://geckoa.lisa.u-pec.fr/, predicts almost exclusive acetyl acetone formation.

Regarding organic nitrates, the infrared spectra clearly show evidence for their formation (as evidenced by absorption features at 1280 and 1660 cm^{-1}, approximately in proportion to their expected relative band strengths). Individual nitrate species cannot be identified or quantified in the IR due to overlapping spectra, and the possibility of absorption due to nitrates other than those targeted here cannot be discounted, but the overall yield obtained is 8±3%. In the GC-FID, four peaks (with retention times in the 6-7.5 min range) display behavior potentially consistent with carbonyl nitrates (based on expected retention times and peak shapes, and their absence in the absence of NOx). Based on observations already described regarding 3-pentanone, and the likelihood that the species $CH_2(ONO_2)C(=O)CH_2CH_2CH_3$ is formed in small yield, our best estimate is that the latter three of the observed four peaks (6.42, 6.8, 7.4 min) are the ones relevant to this analysis (i.e., $-ONO_2$ group on the C3, C4 and C5 positions); their combined yield is 5±3% range, similar to that obtained via IR analysis. Inclusion of all four peaks in the analysis leads to a total yield of 6±3%.

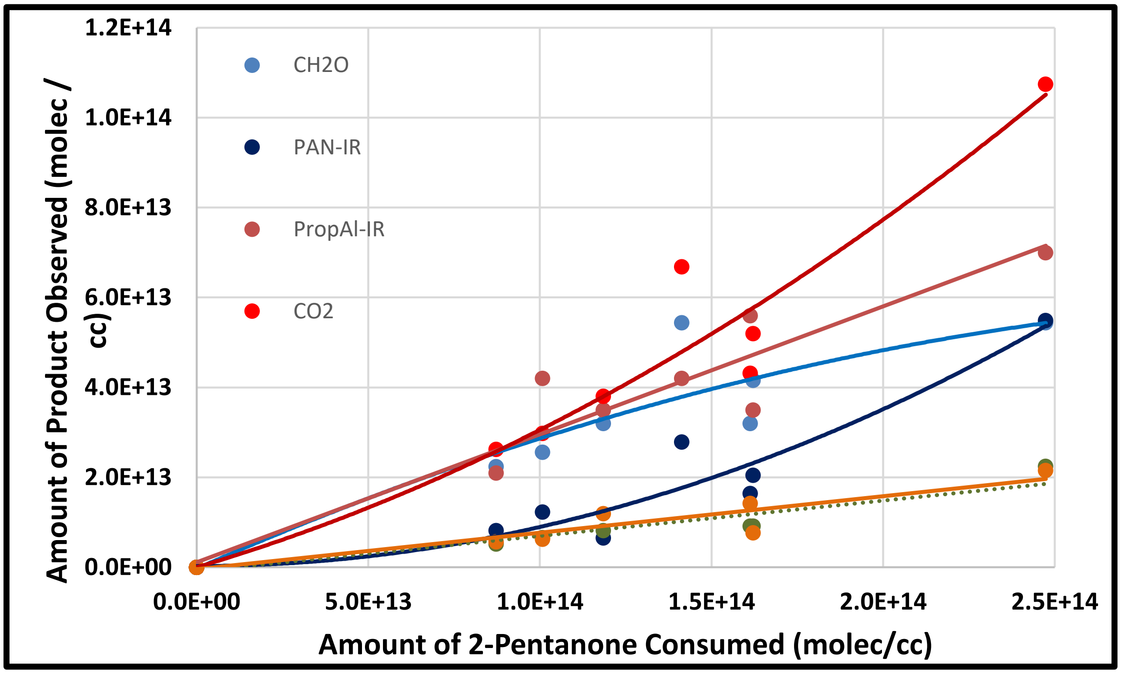

FIGURE 8: Appearance profiles (concentrations of observed products plotted against 2-pentanone consumption) for the major products seen in following photolysis of Cl_2/2-pentanone/NO/O_2/N_2 experiments. Major products observed include CO_2 (red), propanal (orange), formaldehyde (light blue), PAN (darker blue) and total organic nitrates (green and grey, analyzed using two different infrared absorption bands). Nitrate bands were analyzed following subtraction of peaks due to methyl nitrate, PAN and PPN, and thus are subject to considerable uncertainty.

Summary of Findings to Date and Suggestions for Future Work

A summary of observed nitrate production yields from species studied in this work is given in the table below. For the NCAR experiments data are given for both GC/FID and FTIR analysis.

Compound	**Nitrate Yield (%) – GC/FID**		
	CU-Boulder	NCAR (FTIR)	NCAR (GC-FID)
Di-n-octyl ether	15%		
Diethyl Ether		2±2	1±1
Dimethoxy-methane		≈ 2	4±2
Di-isopropyl Ether		3±2	4±2
N-Propyl Ether		8±3	≈ 3%
Ethyl Acetate		6±4	1±1
2-Pentanone		8±3	5±3
3-Pentanone		6±3	3±2

Table 3: Summary of nitrate yields from experiments described in this report. Dioctyl ether experiments were done at CU-Boulder, the remainder at NCAR. At NCAR, yields obtained by FTIR (likely overestimates in some cases) and GC-FID (deemed more reliable) are given separately.

Overarching conclusions from this work can be summarized as follows:

1) Nitrate yields are found in all cases studied to be considerably less, by at least a factor of two and up to about an order of magnitude, than from alkanes containing a similar number of heavy atoms. Thus, local ozone production from oxidation of these types of OVOCs will be larger than is the case for a similarly sized alkane. The work, which directly focused on nitrate yields from these OVOCs, extends and supports a limited number of previous reports in the literature.

2) For a couple of ethers at least, (e.g., dioctyl and diethyl ether), it is clear that the major reduction in nitrate formation is occurring adjacent to the oxygenated functional group.

3) One can see a trend in nitrate formation yields for ethers that extends from about 1% in diethyl ether to 15% in di-octyl ether.

4) In the case of dioctyl ether, the presence of the single O-atom has a profound impact on the outcome of the chemistry, with 78% of the chemistry modified compared to that occurring in a similar-sized alkane. Among the key impacts is the occurrence of more fragmentation, which decreases the secondary organic aerosol formation yield relative to an alkane.

5) In addition to the nitrate yield data, a few additional observations were made that point to inconsistencies in some reaction pathways in detailed atmospheric chemistry mechanisms and mechanism generating systems. For example, the observation of acetic anhydride from oxidation of ethyl acetate (consistent with previous studies in our laboratory) is not captured in any model that we are aware of. Collectively, the data set obtained here should be useful in refining detailed models of atmospheric chemistry (e.g., the Leeds/York MCM, GECKO-A, and SAPRC Mech-Gen).

6) Extension of and decreased uncertainty associated with the data reported here could be obtained via: a) synthesis of as many multifunctional nitrates as possible, to obtain more accurate calibration of their yields and more precise measurements of wall losses, and b) extension of these studies to ‘mid-size’ compounds (e.g., molecules intermediate in size to dipropyl and dioctyl ether) to better establish trends.

REFERENCES

Arey, J., S. M. Aschmann, E. S. C. Kwok, and R. Atkinson, J. Phys. Chem. A, 105, 2001, 1020-1027.

Aumont, B., S. Szopa, and S. Madronich, Atmos. Chem. Phys., 5, 2497-2517, 2005.

Bakker-Arkama, J., and P. Ziemann, *J. Phys. Chem. A* 2021, 125, 26, 5829–5840, https://doi-org.cuucar.idm.oclc.org/10.1021/acs.jpca.1c03688

Bakker-Arkama, J., and P. Ziemann, *ACS Earth Space Chem.* 2021, 5, 3, 690–702, https://doi-org.cuucar.idm.oclc.org/10.1021/acsearthspacechem.1c00008

Carter, W.P. L., J. Jiang, J .J. Orlando, and K. C. Barsanti, Atmos. Chem. Phys., 25, 199-242, 2025, https://doi.org/10.5194/acp-25-199-2025.

Espada, C, and P. B. Shepson**,** Int. J. Chem. Kinet., 37, 2005, 675-685.

Jenkin, M. E., R. Valorso, B. Aumont, and A. R. Rickard, Atmos. Chem. Phys., 19, 2019, 7691-7717, https://doi.org/10.5194/acp-19-7691-2019

Master Chemical Mechanism website, (v3.3.1), https://mcm.york.ac.uk/MCM/,

A. Matsunaga and Ziemann, P. J., Proc. Nat. Acad. Sci, 107, 2009, 6664-6669, https://doi.org/10.1073/pnas.0910585107.

A. Matsunaga and Ziemann, P. J, J. Phys. Chem. A, 107, 2019, 7839-7846, https://doi.org/10.1073/pnas.0910585107.

Orlando, J. J., and G. S. Tyndall, *Int. J. Chem. Kinet.,* **42**, 397-413, 2010, doi: 10.1002/kin.20493.

Orlando, J. J., and G. S. Tyndall, *Chemical Society Reviews*, **41**, 6294-6317, 2012, doi: 10.1039/C2CS35166H.

Teng, A. P., J. D. Crounse, L. Lee, J. M. St. Clari, R. C. Cohen, and P. O. Wennberg, Atmos. Chem. Phys., 15, 4297-4316, 2015, https://doi.org/10.5194/acp-15-4297-2015.

Tyndall, G. S., F. Flocke, Q. Ye, and J. J. Orlando, in preparation, 2025.

Wallington, T. J., M. D. Hurley, J. C. Ball, A. M. Straccia, J. Platz, L. K. Christensen, J. Sehested, O. J. Nielsen, J. Phys. Chem. A, 101, 1997, 5302-5308, DOI: 10.1021/jp9631184.